

INTERNATIONAL WORKSHOP XVI

ON

GROSS PROPERTIES OF NUCLEI AND NUCLEAR EXCITATIONS

HIRSCHEGG, KLEINWALSERTAL, AUSTRIA, JANUARY 18 - 22, 1988

Sponsored by:

BUNDESMINISTER FÜR FORSCHUNG UND TECHNOLOGIE, BONN, FRG

ORGANIZING COMMITTEE:

F. BECK

Institut für Kernphysik, Technische Hochschule  
Schloßgartenstr. 9, D-6100 Darmstadt

H. FELDMIEIER, W. NÖRENBERG

Gesellschaft für Schwerionenforschung mbH  
Postfach 11 05 52, D-6100 Darmstadt

Edited by: HANS FELDMIEIER

ISSN 0720-8715

THE FLUX-TUBE MODEL AND THE PION DECAY OF NONSTRANGE BARYONS

F.I. Stancu and P. Stassart,

Institut de Physique B5, Université de Liège, Sart Tilman,  
B-4000 Liège 1 (Belgium).

The strong coupling Hamiltonian lattice formulation of QCD has led to flux-tube models [1,2] which can be used in the hadron spectroscopy. It has been shown that these models appropriately describe the baryon [3,4,5] and meson [3,6] spectra. The breaking of a flux tube can also provide support [6] for a strong decay mechanism via a quark-pair creation (QPC) model [7,8]. An alternative theoretical foundation of the QPC model of Ref. 8 has also been obtained [9] through a strong coupling and a hopping-parameter expansion. That model refers to the creation of a quark-antiquark pair  $q\bar{q}$  with the vacuum quantum numbers, i.e. in a  $^3P_0$  state. The pair, together with the three quarks forming a resonance R rearranges into a baryon in its ground state N and an emitted meson M.

In a previous work [10], based on the QPC model [8], we have calculated the experimentally known [11] pion decay widths of nonstrange resonances. The present work is viewed as a check and an improvement over two important approximations considered in Ref. 10. One is related to the pion wavefunction and the other to the extension of the flux tube as explained below.

The breaking mechanism of a single flux tube and its application to meson decay has been studied at length in Ref. 6. As compared to the meson, the baryon wavefunction is more complicated. It can be described by two distinct flux tube configurations [1]. One contains three flux tubes emerging from the three quarks and meeting at  $120^\circ$  at a common point  $r_4$  (Fig. 1a). The other appears for interior angles larger than  $120^\circ$ . An example is shown in Fig. 1b. The corresponding flux tube collapses to the common point. In the present work we generalize the single flux breaking mechanism to three flux tubes. Taking an arbitrary point  $r_5$  where the pair creation occurs, we define the total flux-tube-breaking amplitude

$\gamma(\vec{r}_1, \vec{r}_2, \vec{r}_3, \vec{r}_4, \vec{r}_5)$  as the sum of single elementary amplitudes  $\gamma_i$  ( $i = 1, 2, 3$ )

$$\gamma(\vec{r}_1, \vec{r}_2, \vec{r}_3, \vec{r}_4, \vec{r}_5) = \sum_i \gamma_i \quad (1)$$

and assume for  $\gamma_i$  the simple form proposed in Ref. 6

$$\gamma_i = \gamma_0 e^{-\frac{\sqrt{\sigma}}{2\hbar c} d_i^2} \quad (2)$$

where  $\sqrt{\sigma} = 1 \text{ GeV/fm}$  is the string tension constant,  $\gamma_0$  an adjustable parameter and  $d_i$  the shortest distance from  $\vec{r}_5$  to the flux-tube  $i$ . If the perpendicular from  $\vec{r}_5$  to the tube falls outside the length of the tube we define  $d_i$  as the distance to the nearest end, i.e.  $\vec{r}_1$  or  $\vec{r}_4$  which means that we assume the cigar-shaped pair-creation region of Fig. 4b of Ref. 6 although the point  $\vec{r}_4$  is not the location of a color charge.

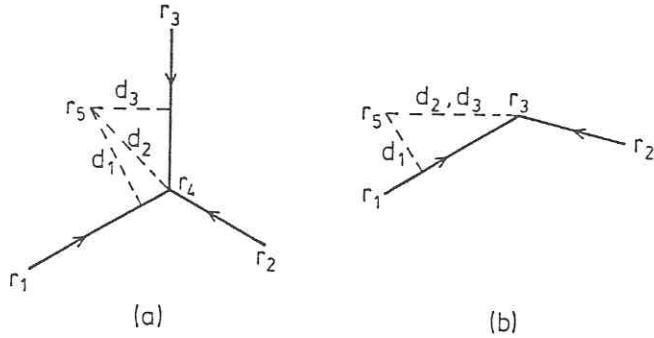


Fig. 1

The common point  $\vec{r}_4$  is uniquely defined by  $\vec{r}_1, \vec{r}_2, \vec{r}_3$  by the requirement of a minimum confining energy. Also, instead of  $r_i$  ( $i = 1, 2, 3$ ) we use the Jacobi coordinates :

$$\vec{\rho} = (\vec{r}_1 - \vec{r}_2)/\sqrt{2} \quad , \quad \vec{\lambda} = (\vec{r}_1 + \vec{r}_2 - 2\vec{r}_3)/\sqrt{6} \quad , \quad \vec{R} = (\vec{r}_1 + \vec{r}_2 + \vec{r}_3)/\sqrt{3} \quad (3)$$

and end up with  $\gamma$  as a function of  $\vec{\rho}, \vec{\lambda}$  and  $\vec{r}_5$ . Then, generalizing the idea of Ref. 6, we define the  $m$ -component  $I_m$  of the pion decay transition amplitude [8] for the process  $R \rightarrow N + M$

trized analytic expression

$$u^\sigma(r) = u^\sigma(0) \exp [-(\gamma_1 r + \gamma_2 r^2)W - \gamma_{1,5} r^{1.5}(1-W)] \quad (7)$$

where

$$u^\sigma(0) = -0.332 \quad ; \quad W = \frac{1 + \exp(-r_0/a)}{1 + \exp((r - r_0)/a)} \quad (8)$$

For the above parameters we found by a  $\chi^2$  fit :  $\gamma_1 = 0.115 \text{ fm}^{-1}$ ,  $\gamma_2 = 10.5 \text{ fm}^{-2}$ ,  $\gamma_{1,5} = 7.0 \text{ fm}^{-3/2}$ ,  $r_0 = 0.72 \text{ fm}$  and  $a = 0.11 \text{ fm}$ . Such an expression has been inspired by the variational forms of Refs. 1,3. The radial part of the pion wavefunction is therefore given by

$$\psi_\pi = f_c(r) s_\pi(r) \quad (9)$$

with  $f_c$  defined in Ref. 3. From the function (9) the pion acquires an rms radius  $\langle r^2 \rangle^{1/2} = 0.16 \text{ fm}$ , i.e. smaller than that of the uncorrelated pion of Ref. 1.

To analyse the role of the pion size and of the extension of the flux tube we display in Table I the square root of decay widths calculated in three different ways. Column 1 lists the resonances. The main components are given in column 2. Column 3 reproduces the results called QPC Set II of Ref. 10, obtained from the QPC model of Ref. 8, i.e. with  $\gamma = ct$  and using the baryon wavefunctions of Ref. 12 (Set II) and the pion wavefunction  $\psi_\pi = f_c$  of Ref. 1. In column 4 we use the pion wavefunction (9) instead of  $f_c$  and the results of column 5 are obtained with  $\psi_\pi$  of Eq. (9) and  $\gamma$  of Eqs. (1), (2), i.e. both  $\psi_\pi$  and  $\gamma$  are different with respect to Ref. 10. Each calculated  $\Gamma^{1/2}$  carries the sign of the corresponding transition amplitude defined according to the conventions of Ref. 13. The negative parity states have pure imaginary amplitudes. The last two columns reproduce the square root of the experimental decay width and the present experimental status [11] of the resonances.

One can see that the better wavefunction (9) of the pion influences considerably the values of those decay widths for which the approximation  $\psi_\pi = f_c$  gave striking disagreements with experiment. These are the  $P_{11}(1440)$ ,  $S_{11}(1650)$ ,  $P_{33}(1600)$  and  $P_{31}(1910)$  resonances, for which now we obtain values within or very near the experimental error. The change

$$\langle NM | \hat{T} | R \rangle = \sum_m \langle 11m - m | 00 \rangle \langle \phi_N \phi_M | \phi_R \phi_{vac}^{-m} \rangle I_m(R; N, M) \quad (4)$$

where the  $\phi$ 's are the flavor-spin wavefunctions as :

$$I_m(R; N, M) = -\sqrt{\frac{3}{4\pi}} \frac{2^3}{(2\pi)^{3/2}} \delta(\vec{k}_M + \vec{k}_N) \int d\vec{\rho} d\vec{\lambda} d\vec{x} d\vec{r}_5 \psi_R(\vec{\rho}, \vec{\lambda} + 2\sqrt{\frac{2}{3}}\vec{x}) \times \psi_N(\vec{\rho}, \vec{\lambda}) e^{i\vec{k}_M(\sqrt{\frac{2}{3}}\vec{\lambda} + \vec{x})} \vec{e}_m \cdot (\vec{k}_M + i\vec{\nabla}_x) \psi_M(2\vec{x}) \gamma(\vec{\rho}, \vec{\lambda}, \vec{r}_5) \quad (5)$$

Here the  $\psi$ 's are the spatial parts of the resonance R, the nucleon N and the pion M wavefunctions. The particular case  $\gamma = ct$  recovers the  ${}^3P_0$  model [8] with  $I_m$  expressed as an integral in the coordinate space [10]. In Ref. 6 it was shown that the  ${}^3P_0$  model corresponds to the limiting case of an infinite extension flux tube, hence  $\gamma = ct$ . With  $\gamma$  defined in Eqs. (1) and (2),  $I_m$  is a 12-dimensional integral while  $\gamma = ct$  reduces it to 9 dimensions. Both are solved by a Monte-Carlo method.

The resonance wavefunctions have been taken from Ref. 12. They have been obtained from the diagonalization of a hyperfine interaction (spin-spin plus tensor) in a truncated space corresponding to the SU(6) supermultiplets  $56(0^+, 2^+)$ ,  $56'(0^+)$ ,  $70(0^+, 1^-, 2^+)$  and  $20(1^+)$  i.e. containing one or two units of angular momentum and one unit of radial excitations. The unperturbed radial states are the flux-tube model variational solutions of Ref. 1.

In Ref. 10, for simplicity reasons, we have used for the pion the variational wavefunction of Ref. 1. This is the solution of a semirelativistic hamiltonian containing a long range confinement and a short range Coulomb potentials. It gives an rms radius  $\langle r^2 \rangle^{\frac{1}{2}} = 0.29$  fm. In Ref. 10 the emission of such a finite size pion has been analysed and compared to a point-like emitted pion. But the magnetic splitting is absent in the above pion wavefunction. That is why in the present work we use a better wavefunction [3] where the effect of the hyperfine interaction is incorporated through a spin-spin short range correlation factor

$$s_{\pi}(r) = 1 - 3 u^{\sigma}(r) \quad (6)$$

with  $u^{\sigma}$  defined by the integral (3.6) of Ref. 3. To reduce the volume of numerical computation we found it useful to express  $u^{\sigma}$  as a parame-

for the  $S_{31}(1620)$  and  $P_{33}(1920)$  goes also in the right direction but there is an unexplained worsening of the agreement for the  $P_{13}(1720)$  resonance. Altogether there is a noticeable reduction of  $\chi^2$  from 106 to 56 where

$$\chi^2 = \sum_i \left[ \frac{\sqrt{\Gamma_i^{th}} - \sqrt{\Gamma_i^{exp}}}{\Delta \sqrt{\Gamma_i^{exp}}} \right]^2 \quad (10)$$

On the other hand, the results of column 5 indicate that the size of the flux tube has little influence on the value of the decay width and therefore  $\gamma = ct$  is a very good approximation. The only significant effect of a finite extension tube is felt on the resonances  $P_{11}(1440)$  and  $P_{33}(1600)$  which are mainly radial excitations. The result for  $P_{33}(1920)$  should be regarded with care because of a very large statistical error in the Monte Carlo method. Generally, for results smaller than unity, there is a large (> 50 %) numerical error.

We would like to thank L. Willets for help in the numerical computation and S. Kumano and J. Kogut for kindly providing the variational parameters of Ref. 3.

#### References :

- [1] J. Carlson, J. Kogut and V.R. Pandharipande, Phys. Rev. D27, 23 (1983).
- [2] N. Isgur and J. Paton, Phys. Rev. D31, 2910 (1985).
- [3] J. Carlson, J. Kogut and V.R. Pandharipande, Phys. Rev. D28, 2808 (1983).
- [4] R. Sartor and Fl. Stancu, Phys. Rev. D31, 128 (1985).
- [5] S. Capstick and N. Isgur, Phys. Rev. D34, 2809 (1986).
- [6] R. Kokoski and N. Isgur, Phys. Rev. D35, 907 (1987).
- [7] L. Micu, Nucl. Phys. B10, 521 (1969) ; R. Carlitz and M. Kislinger, Phys. Rev. D2, 336 (1970).
- [8] A. Le Yaouanc, L. Oliver, O. Pène and J.-C. Raynal, Phys. Rev. 8, 2223 (1973) ; 9, 1415 (1974) ; 11, 1272 (1975).
- [9] H.G. Dosch and D. Gromes, Phys. Rev. D33, 1378 (1986).
- [10] Fl. Stancu and P. Stassart, submitted to Phys. Rev. D. 38(1987)233
- [11] Particle Data Group, Phys. Lett. 170B, 1-350 (1986).
- [12] R. Sartor and Fl. Stancu, Phys. Rev. D34, 3405 (1986).
- [13] R. Koniuk and N. Isgur, Phys. Rev. D21, 1868 (1980).

TABLE I :  $\Gamma_{N\pi}^{\frac{1}{2}}$  (MeV $^{\frac{1}{2}}$ )

Resonance	Main component	$\gamma = ct$ $\psi_{\pi} = F_C$	$\gamma = ct$ $\psi_{\pi}$ eq.(9)	$\gamma$ eq.(1)(2) $\psi_{\pi}$ eq.(9)	Exp.	Status
P <sub>11</sub> (1440)	${}^2N(56^+, 0^+)_{\frac{1}{2}}^{1+}$	+20.8	+12.1	+16.2	10.9 $\begin{matrix} +4.8 \\ -3.2 \end{matrix}$	****
D <sub>13</sub> (1520)	${}^2N(70, 1^-)_{\frac{3}{2}}^{3-}$	+8.4	+7.1	+7.5	8.3 $\begin{matrix} +0.9 \\ -1.2 \end{matrix}$	****
S <sub>11</sub> (1535)	${}^2N(70, 1^-)_{\frac{1}{2}}^{1-}$	+6.3	+9.2	+9.3	8.0 $\begin{matrix} +3.2 \\ -2.1 \end{matrix}$	****
S <sub>11</sub> (1650)	${}^4N(70, 1^-)_{\frac{1}{2}}^{1-}$	+2.3	+7.2	+7.7	9.5 $\begin{matrix} +1.9 \\ -2.1 \end{matrix}$	****
D <sub>15</sub> (1675)	${}^4N(70, 1^-)_{\frac{5}{2}}^{5-}$	+5.6	+5.1	+5.4	7.6 $\begin{matrix} +0.9 \\ -1.1 \end{matrix}$	****
F <sub>15</sub> (1680)	${}^2N(56, 2^+)_{\frac{5}{2}}^{5+}$	+9.7	+7.5	+8.5	8.7 $\begin{matrix} +0.8 \\ -0.9 \end{matrix}$	****
D <sub>13</sub> (1700)	${}^4N(70, 1^-)_{\frac{3}{2}}^{3-}$	-4.1	-3.6	-3.9	3.2 $\begin{matrix} +1.0 \\ -1.3 \end{matrix}$	***
P <sub>11</sub> (1710)	${}^2N(70, 0^+)_{\frac{1}{2}}^{1+}$	+1.8	-3.7	-3.1	4.0 $\begin{matrix} +1.1 \\ -1.0 \end{matrix}$	***
P <sub>13</sub> (1720)	${}^2N(56, 2^+)_{\frac{3}{2}}^{3+}$	-7.1	-11.0	-11.7	5.4 $\begin{matrix} +1.7 \\ -1.9 \end{matrix}$	****
F <sub>17</sub> (1990)	${}^4N(70, 2^+)_{\frac{7}{2}}^{7+}$	-1.8	-1.1	-1.2	4.2 $\begin{matrix} +1.9 \\ -2.1 \end{matrix}$	**
F <sub>15</sub> (2000)	${}^4N(70, 2^+)_{\frac{5}{2}}^{5+}$	-2.0	-1.8	-1.7	1.9 $\begin{matrix} +0.7 \\ -0.7 \end{matrix}$	**
P <sub>33</sub> (1232)	${}^4\Delta(56, 0^+)_{\frac{3}{2}}^{3+}$	+10.7	+10.7	+10.7	10.7 $\begin{matrix} +0.2 \\ -0.2 \end{matrix}$	****
P <sub>33</sub> (1600)	${}^4\Delta(56^+, 0^+)_{\frac{3}{2}}^{3+}$	-0.2	-7.4	-4.1	7.0 $\begin{matrix} +2.4 \\ -1.8 \end{matrix}$	**
S <sub>31</sub> (1620)	${}^2\Delta(70, 1^-)_{\frac{1}{2}}^{1-}$	-0.6	-2.8	-2.9	6.5 $\begin{matrix} +1.0 \\ -1.0 \end{matrix}$	****
D <sub>33</sub> (1700)	${}^2\Delta(70, 1^-)_{\frac{3}{2}}^{3-}$	-4.8	-4.3	-4.5	6.1 $\begin{matrix} +1.6 \\ -1.7 \end{matrix}$	****
F <sub>35</sub> (1905)	${}^2\Delta(70, 2^+)_{\frac{5}{2}}^{5+}$	+3.1	+2.1	+2.3	5.5 $\begin{matrix} +2.2 \\ -2.0 \end{matrix}$	****
P <sub>31</sub> (1910)	${}^2\Delta(70, 0^+)_{\frac{1}{2}}^{1+}$	+0.7	+5.4	+6.0	6.6 $\begin{matrix} +2.5 \\ -1.1 \end{matrix}$	****
P <sub>33</sub> (1920)	${}^4\Delta(56, 2^+)_{\frac{3}{2}}^{3+}$	+2.0	+2.4	+0.5	6.6 $\begin{matrix} +1.1 \\ -1.3 \end{matrix}$	***
F <sub>37</sub> (1950)	${}^4\Delta(56, 2^+)_{\frac{7}{2}}^{7+}$	-8.7	-6.6	-7.2	9.8 $\begin{matrix} +2.6 \\ -1.4 \end{matrix}$	****